Size effects in the nonlinear resistance and flux creep in a virtual Berezinskii-Kosterlitz-Thouless state of superconducting films.

A. Gurevich[1] and V.M. Vinokur[2].

[1]National High Magnetic Field Laboratory, Florida State University, Tallahassee, Florida, 32310
[2]Materials Science Division, Argonne National Laboratory, Argonne, Illinois, 60439
(Dated: September 7, 2018)

We show that the size effects radically affect the electric field-current $(E-I)$ relation of super-conducting films. We calculate $E(J)$ due to thermally-activated hopping of single vortices driven by current I across the film in a magnetic field H, taking into account interaction of free vortices with their antivortex images and peaks in the Meissner currents at the film edges. Unbinding of virtual vortex-antivortex pairs not only mimics the transport uniform BKT behavior, it can dominate the observed $E(J)$ and result in the field-dependent ohmic resistance at small I. We show that $E(I)$ can be tuned by changing the film geometry and propose experimental tests of this theory.

The Berezinskii-Kosterletz-Thouless (BKT) transition is a 2D universal phase transition due to unbinding of logarithmically interacting topological excitations [1]. The concept of the BKT transition first introduced in the context of vortices in XY-magnets has been extended to other topological excitations like vortex-antivortex pairs in superfluid films, superconducting films, Josephson-junction arrays [2, 3], dislocation pairs in the theory of 2D melting or ultracold atomic gases in optical lattices [4]. The superconducting films and Josephson arrays have become the main experimental testbeds to study the BKT transition by dc transport measurements. In this case the ohmic electric field-current characteristics $R = RI$ above the transition $T > T_{BKT}$ turns into the power-law $E \propto I^{1+\alpha}$ at $T < T_{BKT}$ with a jump to $\alpha = 2-5$ followed by the growth of α as the temperature T decreases [3].

While the interaction of dislocations and vortices in XY-magnets of superfluid films is indeed logarithmic, the interaction of vortices in superconducting films is only logarithmic over distances shorter than the Pearl screening length $\Lambda = \lambda^2/d$ where d is the film thickness and λ is the London penetration depth [5]. The size effects can change the BKT transport behavior at $T < T_{BKT}$ since the result, $E \propto I^{1+\alpha}$, holds only at sufficiently high currents, $I > I_1 \sim c\epsilon/\phi_0$, for which the critical size of a dissociating vortex-antivortex pair, $\ell_c = 2cw\epsilon/\phi_0 I$, is smaller than the film width, w, where $\alpha = 2\epsilon/T$, $\epsilon = \phi_0^2/16\pi^2\Lambda$ is the vortex energy scale, ϕ_0 is the flux quantum, and c is the speed of light. For $I < I_1$, the $E - I$ characteristic becomes ohmic [2, 3, 6, 7, 8]. Yet several crucial features of the electrodynamics of superconducting films have not been incorporated into the BKT theory. First, the sheet current density $J(x)$, which drives vortices across the film can be highly nonuniform. For a current-carrying thin film strip of width $w > \Lambda$ in a perpendicular magnetic field H, we have [9]:

$$J(x) = [I + (w - 2x)Hc/4]/\pi\sqrt{x(w-x)}, \quad (1)$$
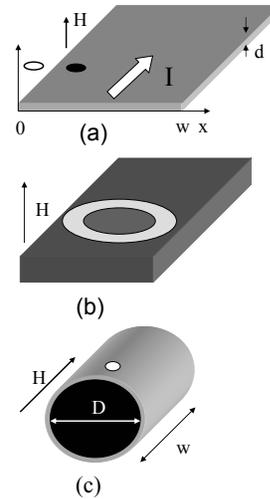
where the geometry is shown in Fig. 1a. This distribu-

FIG. 1: A thin film in a perpendicular field H. The black dot shows a vortex moving across the film, and the empty circle shows the antivortex image (a). Geometries for probing the resistive state by relaxation measurements: a thin ring in a perpendicular field (b), and a thin tube on a cylindrical substrate in a parallel field (c). The white dot shows the vortex driven along the tube by the azimuthal Meissner currents.

tion of $J(x)$ ensures no spontaneous vortices generated by small I and H in the film (the singularities at the film edges are cut off at the distances $\sim \max(d, \lambda)$). The second feature results from the Bean-Livingston surface barrier: a vortex penetrating a film interacts with a fictitious antivortex image, which provides zero normal currents at the edges. Thus, thermally-activated penetration of single vortices is governed by the BKT-type unbinding of a virtual vortex - antivortex pair [6]. For $w < \Lambda$, the interaction energy $U(\mathbf{r_1}, \mathbf{r_2})$ between two vortices is logarithmic only for small separation, $|\mathbf{r_1}-\mathbf{r_2}| < w$, otherwise $U(\mathbf{r_1}, \mathbf{r_2})$ decays exponentially over the length w/π along the film because of cancelation of the vortex currents by an infinite chain of vortex-antivortex images [10]. This

makes rare thermally-activated hops of vortices across the strip uncorrelated at low T and I.

In this Letter we show that fluxon hopping mediated by the unbinding of a vortex from its edge antivortex images mimics the uniform BKT resistive state and results in a strongly size-dependent $E(I)$, which can exceed $E_2(I)$ caused by the uniform pair dissociation [2] both for $w < \Lambda$ and $w > \Lambda$. This is due to the fact that the energy activation barrier for the single vortex penetration is roughly half of the barrier required to create a vortex-antivortex pair in the film. The account of these features is important for the interpretation of deviations from the BKT scenario and critical currents observed on $E - I$ curves of ultrathin films [11, 12, 13, 14]. Since it is the thin film strip geometry, which is mostly used in dc transport measurements, we also discuss other geometries in which the genuine BKT pair dissociation could be revealed.

We calculate $E(I)$ due to vortex hopping across a thin film described by the Langevin equation $\eta\dot{x} + U'(x) = \zeta$ where the dot and the prime denote differentiations over time t and coordinate x, respectively, η is the viscous drag coefficient, $\zeta(t)$ describes thermal noise and the local energy $U(x) = U_0 - U_m$ comprises the position-dependent vortex self-energy $U_0(x)$ and the work of the Meissner current, $U_m = (\phi_0/c)\int_0^x J(u)du$ to move the vortex by the distance x from the film edge. Here $J(x)$ is described by the integral Maxwell-London equation [5, 9]

$$\int_0^w \frac{J(u)du}{u-x} + 4\pi\Lambda\partial_x J = -cH \tag{2}$$

supplemented by the condition $I = \int_0^w J(x)dx$. If $w \gg \Lambda$, Eq. (2) yields Eq. (1), but for $w \ll \Lambda$, the integral term is negligible, and $J(x) \simeq I/w + cH(w-2x)/8\pi\Lambda$.

The self-energy $U_0(x) = -\int_0^x F(u)du$ is the work required to create a vortex at the edge where $U_0(0) = 0$ and move it by the distance x. Here $F(x) = f(2x) + \sum_{n=1}^\infty [f(2wn + 2x) - f(2wn - 2x)]$ is the force between the vortex in the film and an infinite chain of vortex and antivortex images outside the film, $f(x) = \phi_0 J_y(x)/c$, and $J_y(x)$ is the y-component of the sheet current density of the Pearl vortex in an infinite film. Using $J_y(k) = -ic\phi_0 k_x/2\pi k(1+2\Lambda k)$, $k^2 = k_x^2 + k_y^2$ [5] and integrating over k_y in the Fourier space, we obtain:

$$U_0 = \frac{\phi_0^2}{\pi^2}\sum_{n=1}^N \frac{\sin^2(\pi nx/w)}{\sqrt{(2\pi n\Lambda)^2 - w^2}}\tan^{-1}\left[\frac{2\pi n\Lambda - w}{2\pi n\Lambda + w}\right]^{1/2} \tag{3}$$

Here $N \simeq we^{-C}/2\pi\xi$ and $C = 0.577$ provide the vortex core cutoff. For narrow films $w \ll 2\pi\Lambda$, the summation in Eq. (3) reproduces the known result [10, 15]:

$$U_0(x) = \epsilon\ln[(w/\pi\xi)\sin(\pi x/w)], \tag{4}$$

where $\epsilon = \phi_0^2/16\pi^2\Lambda$. Here U_0 results from the kinetic energy of unscreened vortex supercurrents cut off at the
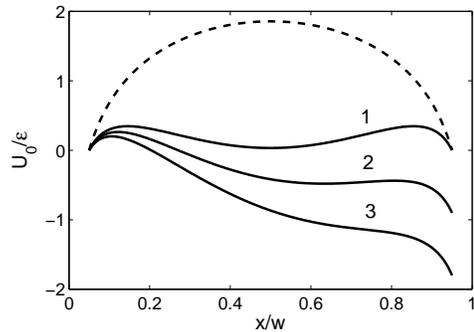

FIG. 2: The vortex energy $U(x)$ given by Eqs. (4) and (6) for a strip with $w \ll \Lambda$ and $w = 20\xi$. The dashed line shows $U_0(x)$, and the solid lines show $U(x)$ for $H\phi_0 w^2/8\pi\Lambda\epsilon = 9$ and different currents, $\phi_0 I/c\epsilon$: 0 (1); 1 (2), and 2 (3).

distance $\sim \xi$ from the edges where the London theory breaks down. For wide films $w > 2\pi\Lambda$, $U_0(x)$ increases from zero at $x = 0$ to $U_a \simeq \epsilon\ln(\Lambda/\xi)$ over the length $x \sim \Lambda$. The magnetic part of the energy barrier $U_m(x)$ for $w \gg \Lambda$ and $w \ll \Lambda$, is given by

$$U_m = \frac{2\phi_0 I}{\pi c}\sin^{-1}\sqrt{x/w} + \frac{\phi_0 H}{2\pi}\sqrt{x(w-x)}, \quad w \gg \Lambda \tag{5}$$

$$U_m = \phi_0 Ix/cw + \phi_0 Hx(w-x)/8\pi\Lambda, \quad w \ll \Lambda \tag{6}$$

The behavior of $U(x)$ at different I and H is shown in Fig. 2. The transport current tilts $U(x)$, reducing the barrier maximum and shifting its position $x_0(I)$ toward the film edge. The barrier disappears at $I = I_s$ for which $x_0(I_s) \sim \xi$. In turn, the magnetic field at $I = 0$ leaves $U(x)$ symmetric, but can produce a minimum in $U(x)$ at $x = w/2$. There are 3 characteristic fields: H_b at which the minimum in $U(x)$ appears, the lower critical field H_{c1} at which $U(w/2) = 0$, and H_s, at which the edge barrier disappears. These critical currents and fields can be calculated from the equation $U'(x_0) = 0$.

We calculate $E(I)$ for $T < T_{BKT}$, $H < H_{c1}(I)$ and $I < I_s(H)$ so that the voltage V results from thermally-activated hopping of vortices and antivortices over the barrier $U^\pm(x) = U_0 - U_m^\pm$. Here $U_m^-(x)$ for antivortices is given by Eq. (5) with $H \to -H$ and $\sin^{-1}(x/w)^{1/2} \to \cos^{-1}(x/w)^{1/2}$ or by Eq. (6) with $H \to -H$ and $x \to w - x$. The mean drift velocities $v_\pm$ of vortices and antivortices follow from the solution of the Fokker-Planck equation with a constant probability current [16]:

$$1 \simeq \frac{\eta v_\pm}{wT[F_\pm(w) - F_\pm(0)]}\int_\xi^{w-\xi}dxF_\pm(x)\times$$
$$\left[\int_0^x dy\frac{F_\pm(0)}{F_\pm(y)} + \int_x^w dy\frac{F_\pm(w)}{F_\pm(y)}\right] \tag{7}$$

where $\beta = \epsilon/T$, $F_\pm(x) = \exp[(U_m^\pm(x) - U_0(x))/T]$, so that $F_+(0) = F_-(w) = 1$, and $F_+(w) = F_-(0) = $

$\exp(\phi_0 I/cT)$. The integral over x is cut off on the scales of the vortex core size, and the condition $T < T_{BKT}$ implies that $\beta > 2$. If $I \ll I_s$, where I_s for $w \ll \Lambda$ is of the order of the depairing current, the x-integral is determined by the vicinity of the edges. Indeed, for $x \approx 0$, the self-energy $U_0(x) \simeq \epsilon \ln(x/\xi)$ is dominated by interaction of the vortex with the nearest image, thus $F(x) \approx (\xi/x)^\beta F(0)$, the first y-integral in the brackets is negligible and the lower limit of the second y-integral can be set to $x = 0$. Doing the same for $x \approx w$, we obtain the factor $2F(0)F(w)\xi/(\beta-1)$ after integration over x.

The velocities $v_\pm$ are proportional to the mean electric field $E \simeq \phi_0(v_+ - v_-)/wc\xi$. This follows from the Joule power $IV = \phi_0 I(v_+ - v_-)L/\xi wc$ produced by the driving force $I\phi_0/wc$ to move a vortex across the film and multiplied by the number $\simeq L/\xi$ of statistically-independent edge sites available for uncorrelated vortex entries in the strip of length L. Using the Bardeen-Stephen expression for $\eta \simeq d\phi_0^2/2\pi\xi^2 c^2\rho_n$ in Eq. (7), we obtain [17]

$$E = \frac{\pi c\rho_n T(\beta-1)}{d\phi_0}\left[1 - e^{-I\phi_0/cT}\right]\left[Z_+^{-1} + Z_-^{-1}\right], \quad (8)$$

$$Z_\pm = \int_0^w e^{U^\pm/T}dx. \quad (9)$$

The behavior of $E(I,T,H)$ described by Eq. (8) is shown in Fig. 3: $E(I)$ is ohmic for $I\phi_0 \ll cT$ and nonlinear at higher I. The ohmic $E = R_v I$ at $H = 0$ is quantified by the Arrhenius-type resistance $R_v \propto (-U_a/T)$ per unit length, for which Eqs. (4), (8) and (9) give:

$$R_v = \frac{2\pi^{3/2}\beta\rho_n\Gamma(\beta/2)}{dw\Gamma[(\beta-1)/2]}\left(\frac{\pi\xi}{w}\right)^\beta, \qquad w \ll \Lambda \quad (10)$$

where $\Gamma(x)$ is the gamma-function. The barrier hight, $U_a = \epsilon\ln(w/\pi\xi) = U_0(w/2)$ depends logarithmically on w in accordance with Eq. (4). For $\beta \gg 1$, Eq. (10) yields $R_v \simeq (\sqrt{2}\rho_n/dw)(\pi\beta)^{3/2}(\pi\xi/w)^\beta$, much smaller than the normal resistance $R_n = \rho_n/dw$. In wide films $w \gg \Lambda$, the barrier $U_a \simeq \epsilon\ln(\Lambda/\xi)$ becomes independent of w.

For $2\phi_0 I > \pi cT$, or $\phi_0 Hw > 2\pi T$ the change of the barrier shape $U(x)$ shown in Fig. 2 results in a strongly nonlinear and field dependent $E(I,H)$, which can be calculated numerically from Eqs. (2) and (8) for any ratio w/Λ, and analytically for both limits $w \ll \Lambda$ and $w \gg \Lambda$. For instance, in wide films at $I_s\xi/\sqrt{dw} \ll I \ll I_s$, the fluxon hopping is limited by the small barriers near the edges: $U^+(x) \simeq \epsilon\ln(x/\xi) - \phi_0(2I/\pi c + Hw/2\pi)\sqrt{x/w}$ at $x \ll w$. For $H \gg 2\pi T/w\phi_0$, the antivortex channel is suppressed, $Z_+ \ll Z_-$, so Eqs. (8) and (9) yield:

$$E = \frac{\pi\rho_n cT(\beta-1)(\xi/w)^\beta}{2dw\phi_0\Gamma(2\beta+2)}\left[\frac{\phi_0}{\pi T}\left(\frac{2I}{c} + \frac{Hw}{2}\right)\right]^{2\beta+2} \quad (11)$$

In the limit $I\phi_0 \ll cT$, but $H\phi_0 w \gg 2\pi T$, the ohmic

resistance R_v strongly depends on H:

$$R_v \simeq \frac{\pi\rho_n(\beta-1)}{2dw\Gamma(2\beta+2)}\left(\frac{\xi}{w}\right)^\beta\left(\frac{\phi_0 Hw}{2\pi T}\right)^{2\beta+2}. \quad (12)$$

For $H \ll 4I/c$, but $2I\phi_0 \gg \pi cT$, the vortex and antivortex channels yield the power-law $E(I)$:

$$E = \frac{\pi\rho_n cT(\beta-1)}{dw\phi_0\Gamma(2\beta+2)}\left(\frac{\xi}{w}\right)^\beta\left(\frac{2\phi_0 I}{\pi cT}\right)^{2\beta+2}. \quad (13)$$

For narrow film $w \ll \Lambda$ at $H = 0$, the integral in Eq. (9) can be evaluated analytically for all $I < I_s$:

$$E = \frac{4\pi\rho_n cT(\beta-1)}{d\phi_0 w\Gamma(\beta+1)}\left[\frac{2\pi\xi}{w}\right]^\beta\left|\Gamma\left(1 + \frac{\beta}{2} + i\gamma\right)\right|^2\sinh\pi\gamma \quad (14)$$

where $\gamma = \phi_0 I/2\pi cT$. In the limit $\gamma \ll 1$, Eq. (14) reproduces Eq. (10), but for $\gamma \gg \beta/2$, that is, $J_0\xi/w \ll J < J_0$ where $J_0 = c\phi_0/8\pi^2 e\Lambda\xi$ is of the order of the sheet depairing current density, Eq. (14) gives

$$E = \frac{2\pi\rho_n(\beta-1)}{d\Gamma(\beta+1)}\left(\frac{\phi_0\xi J}{cT}\right)^\beta J. \quad (15)$$

This power-law $E(J)$ can also be obtained in the same way as Eq. (13) by expanding $U(x)$ near the film edges. Notice that $E(J)$ given by Eq. (15) is independent of w because, once the vortex overcomes a narrow ($\ll w$) edge barrier shown in Fig. 2, its subsequent viscous motion across the film is no longer thermally-activated.

It is instructive to compare Eqs. (13) and (15) with the electric field $E_2 \sim (\rho_n J/d)(J/J_0)^{2\beta}$ produced by the uniform BKT dissociation of vortex-antivortex pairs above the critical size $\ell_c = 2\epsilon c/\phi_0 J$ [2]. For narrow films at low temperatures, $(w \ll \Lambda, \beta \gg 1)$, we can use $\Gamma(z) \simeq (2\pi/z)^{1/2}e^{-z}z^z$ in Eq. (15) and obtain

$$E_2/E \sim (J/2J_0)^\beta/e\sqrt{2\pi\beta} \quad (16)$$

Hence, for $\beta \gg 1$, the virtual vortex-image unbinding dominates over the uniform pair dissociation except in the region $T \approx T_{BTK}$ of the genuine BKT behavior. In wide films, the single-vortex contribution $E/E_2 \sim (w/\xi)^\beta \gg 1$ is further enhanced by the singularities of the Meissner current at the edges. As an illustration Fig. 3 shows $E(I)$ calculated from Eq. (8), which gives $E > (10^2 - 10^3)E_2$ in the region where $\ell_c < w$. Moreover, $E(I)$ due to the edge vortex-image unbinding exhibits all characteristic features of the BKT nonlinear transport in a finite size film: the ohmic $E(J)$ below the critical current I_c followed by the power-law $E = RJ(J/J_0)^{\alpha_1}$ for $I > I_c$. Here the exponent α_1 varies from $\alpha_1 = 2\beta + 1$ for wide films to $\alpha_1 = \beta$ for narrow films, while the uniform pair unbinding gives $\alpha_2 = 2\beta$ [2]. The similarity of α_1 and α_2 in wide films results from the edge Meissner singularity of $J(x)$, which increases α_1 as compared to
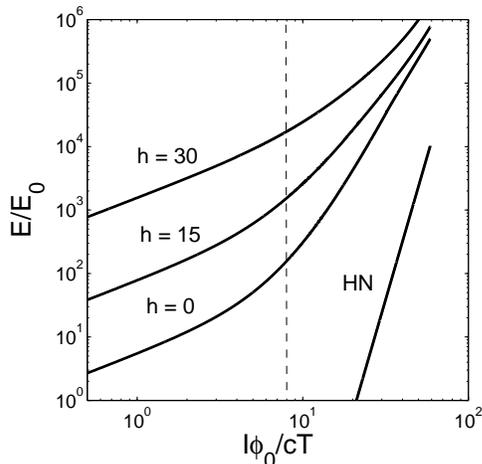
FIG. 3: $E - J$ curves calculated from Eq. (8) for $\beta = 4$, $w = 20\xi \ll \Lambda$ and different fields $h = H\phi_0 w^2/8\pi\Lambda T$. Here $j = I\phi_0/cT < j_s = 2\beta w/e\xi$, and $E_0 = \pi c\rho_n T(\beta - 1)(\pi\xi/w)^\beta/dw\phi_0$. The line labeled by HN shows the Halperin-Nelson result, $E_2(I)$ [2]. The critical pair length ℓ_c exceeds w in the region $j < 2\beta$ left of the dashed line.

$\alpha_1 = \beta$ for a uniform J. The critical current I_c is estimated from the condition that the maximum of $U(x)$ at $x = x_0(I)$ shifts from the film center at $I \ll I_c$ to the edge at $x_0 \ll w$ for $I \gg I_c$. For a narrow film, I_c defined by $x_0(I_c) = w/4$ in Eqs. (4) and (6) is:

$$I_c(H) = \frac{c\phi_0}{16\pi\Lambda}\left(1 - \frac{H}{H_0}\right), \qquad H_0 = \frac{\phi_0}{w^2}, \qquad (17)$$

so that $I_c(0)$ is independent of w, but both $J_c(0) = I_c/w \sim J_0\xi/w$ and H_0 increase as w decreases. The same $I_c(0) = \pi c\epsilon/\phi_0$ is obtained, defining the nonlinearity onset from the condition $l_c = 2w/\pi$ equivalent to $\gamma = \beta/2$ in the argument of the gamma-function in Eq. (14).

The results presented above indicate that $E(J)$ can be tuned by changing the film geometry. For instance, if a uniform $J(x)$ is produced in a wide film, the exponent $\alpha_1 = 2\beta + 1$ would decrease to $\alpha_1 = \beta$. This could be implemented by using ferromagnetic/superconducting structures [15, 18], in which a thin film strip is placed perpendicular to ferromagnetic screens to eliminate the singularity in $J(x)$ [18]. Another possibility is to use a thin film tube in a parallel field, which produces uniform azimuthal screening currents $J = cHd/4\pi\lambda$ driving vortices along the tube. Because of the negligible demagnetization factor of this geometry, $J(x)$ for large tubes of length $L \gg \Lambda$ and diameter $D \gg \Lambda$ does not contain the Meissner edge singularities characteristic of wide films in a perpendicular field. Such a tube would have a mixed $E(J)$ controlled by $U_0(x)$ of a wide strip, but a uniform current drive like in a narrow film.

Film and ring structures make it possible to probe $E(J)$ by magnetic relaxation measurements well below the nV voltage sensitivity [11] of transport measurements. In this case $H(t)$ is ramped up and then stopped, after which the magnetic moment $M(t) = I(t)D/2c$ is measured. For $\mathcal{L}I \gg \phi_0 c$, relaxation of $I(t)$ in a ring or a tube is described by the circuit equation $\mathcal{L}\dot{I} = -\pi c^2 DRI(I/I_0)^\alpha$, where $\mathcal{L}$ is the self-inductance. The solution of this equation, $I(t) = (\tau/t)^\alpha I_0$ with $\tau = \mathcal{L}/\pi c^2 DR\alpha$, enables extracting $\alpha(T)$ from flux creep measurements after some initial transient time [19].

In conclusion, thermally-activated fluxon hopping mediated by unbinding of single vortices from their edge antivortex images can mimic the nonlinear resistive behavior of a uniform BKT state. Our results predict a strong dependence of $E(J, H, T)$ on temperature, magnetic field and the sample size. This offers a possibility of tuning the behavior of $E(J)$ by changing the film geometry or by incorporating magnetic structures.

[1] V.L. Berezinskii, Zh. Exp. Teor. Fiz. **61**, 1144 (1971) [Sov. Phys. JETP **34**, 610 (1972)]; J.M. Kosterlitz and J.D. Thouless, J. Phys. C**6**, 1181 (1973).
[2] B.I. Halperin and D.R. Nelson, J. Low Temp. Phys. **36**, 599 (1979); S. Doniach and B.A. Huberman, Phys. Rev. Lett. **42**, 1169 (1979).
[3] P. Minnhagen, Rev. Mod. Phys. **59**, 1001 (1987).
[4] Z. Hadzibabic et al., Nature **441**, 1118 (2006).
[5] J. Pearl, Appl. Phys. Lett. **5**, 65 (1964).
[6] V. Ambegaokar, B.I. Halperin, D.R. Nelson, and E.D. Siggia, Phys. Rev. B **21**, 1806 (1980).
[7] S.W. Pierson et al., Phys. Rev. B **60**, 1309 (1999); K. Medvedeva et al., Phys. Rev. B **62**, 14531 (2000).
[8] L. Benfatto, C. Castellani, and T. Giamarchi, Phys. Rev. Lett. **99**, 207002 (2007).
[9] E. Zeldov et al., Phys. Rev. Lett. **73**, 1428 (1994); E.H. Brandt and G.P. Mikitik, ibid. **85**, 4164 (2000).
[10] G. Stejic et al., Phys. Rev. B **49**, 1274 (1994). In this paper the GL vortex core energy in Eq. (4) is taken into account by the renormalization of the bulk coherence length ξ_0 to $\xi = e^{-0.38}\xi_0/2 \simeq 0.34\xi_0$.
[11] J.M. Repaci et al., Phys. Rev. B **54**, R9674 (1996); D.R. Strachan, C.J. Lobb, and R.S. Newrock, Phys. Rev. B **67**, 174517 (2001).
[12] M.M. Ozer et al., Phys. Rev. B **74**, 235427 (2006); Science **316**, 1594 (2007).
[13] A. Rüfenacht et al., Phys. Rev. Lett. **96**, 227002 (2006).
[14] F. Tafuri et al., Europhys. Lett. **73**, 948 (2007).
[15] V.G. Kogan, Phys. Rev. B **75**, 064515 (2007).
[16] V. Ambegaokar and B.I. Halperin, Phys. Rev. Lett. **22**, 1364 (1969).

[17] A more rigorous treatment of the core cutoff may produce a factor ~ 1 in Eq. (8), which does not change the behavior of $E(I, T, H)$. The entry barrier is also affected by the rounding of the film edge, J.R. Clem, R.P. Huebener, and D.E. Gallus, J. Low Temp. Phys. **12**, 449 (1973).

[18] Yu. A. Genenko, A. Snezhko, and H.S. Freyhardt, Phys. Rev. B **62**, 3453 (2000); I.F. Lyuksytov and V.L. Pokrovsky, Adv. Phys. **54**, 67 (2005).

[19] A. Gurevich, Int. J. Mod. Phys. B**9**, 1045 (1995).